International Journal of Innovative Computing, Information and Control
Volume **13**, Number **2**, April **2017**

ICIC International ©2017 ISSN 1349-4198
pp. 453–470

MIMO FUZZY LOGIC SUPERVISOR-BASED ADAPTIVE CONTROL USING THE EXAMPLE OF COUPLED-TANKS LEVELS CONTROL

Snejana Yordanova[1], Vladimir Yankov[1] and Lakhmi Jain[2]

[1]Department of Continuous Processes Control
Technical University of Sofia
8 Kliment Ohridski blvd., Sofia 1000, Bulgaria
sty@tu-sofia.bg; vladimir_qnkov@abv.bg

[2]Faculty of Education, Science, Technology and Mathematics
University of Canberra
Canberra, ACT 2601, Australia
Lakhmi.Jain@canberra.edu.au

Received September 2016; revised January 2017

Abstract. *Fuzzy logic (FL) controllers (FLCs) ensure stable and robust control of multi-input multi-output (MIMO) nonlinear industrial processes with no reliable models. To respond to the plant changes and the requirements of industrial implementation, a design approach is suggested for computationally simple MIMO FL supervisor-based adaptive FLCs (SAFLCs) suitable for use by programmable logic controllers (PLCs). The SAFLC consists of a main model-free MIMO FLC and a MIMO FL supervisor (FLS) for keeping desired system performance by on-line adaption of the FLC's scaling factors. The real-time plant control by the empirically designed FLC provides data for the derivation via genetic algorithms (GAs) of a transfer matrix-based Takagi-Sugeno-Kang (TSK) plant model and for its validation. The TSK plant model enables computational system sensitivity analysis for the design of the optimal structure MIMO FLS. The SAFLC is approximated to a simple PLC feasible parallel distributed compensation (PDC) using GAs and real-time plant control data used also for the PDC validation. The Lyapunov SAFLC system stability is studied via the TSK-PDC system representation and linear matrix inequalities. The designed SAFLC real-time control of coupled levels reduces the system settling time, overshoot and coupling in comparison to the FLC control.*
Keywords: Coupled levels, Fuzzy logic, Fuzzy supervisor adaptation, Lyapunov stability, Multivariable, Real-time control

1. **Introduction.** The high performance demands for the control of various processes in the modern complex installations (boilers, evaporators, reactors, distillation columns, etc.) reveal the necessity to account for the plant nonlinear, multi-input multi-output (MIMO) and inertial character, the disturbances and the changes of its characteristics in time or with the operation point. Such plants are difficult to be modelled and controlled by classical approaches [1]. The fuzzy logic controllers (FLCs) tackle successfully these control problems by simple means and a model-free design combining expert knowledge with measurements for ensuring system stability and robustness. Their adaptation and auto-tuning are enhanced by integrating the FLC [2,3] with the adaptive theory principles [4] in an adaptive FLC (AFLC). The AFLC tunes the main controller's gains and scaling factors (ScFs) in *fuzzy self-tuning control* affecting uniformly the FLC gains, resolution and membership functions (MFs) universes of discourse [5-9]. The algorithm is easily embedded in microcontrollers [6] and programmable logic controllers (PLCs) for

real-time operation [8]. The AFLCs can also tune the MFs – mainly the peaks, for influencing specific areas of the control surface, or the rule base via the rule consequents, often singletons, or the rule-base relation matrix in *fuzzy self-organizing control* [10-15]. *Fuzzy model reference learning controllers* use a reference model to set the system performance requirements and an adaptation mechanism, built of a fuzzy inverse model and a knowledge-based modifier [3,16-19]. *Fuzzy gain scheduling* AFLCs [20] tune ScFs or/and switch between rule tables with the effect of adaptation of MFs and fuzzy rules. They are easily implemented in PLCs. Recently, *approximation-based adaptive FLCs* have been developed with proven system global asymptotic stability [21,22].

A simple *fuzzy logic (FL) supervisor* (FLS) from a second control level can be easily designed using little knowledge about the plant to continuously and nonlinearly auto-tune the main controller to keep on-line estimated performance indicators to their expert defined norm terms [3,9,23-26]. The FLS has performance measures as inputs and therefore it is considered a modification of the direct AFLC [3,4,9,27]. The necessary local modifications in the control surface can be ensured by adjustment of ScFs and gains, present in any type of main controller. The effect is equivalent to the application of complicated techniques of tuning of rules and MFs [27].

The development of supervisor-based AFLCs (SAFLCs) still lacks a systematic design methodology that considers multi-input multi-output (MIMO) industrial processes, system stability, optimal SAFLC structure, reduced computational effort to enable broad industrial applications in noisy environment and in real-time operation via PLC and is based on real-time experimentation data rather than on simulations.

The aim of the present paper is to develop such a systematic approach for the design of simple model-free MIMO supervisor-based AFLCs that ensures the closed loop system stability and high performance and a PLC feasibility of the controller. It is implemented for the real-time adaptive FLC of the liquid levels in a laboratory-scale coupled-tank system using MATLAB^{TM} [28,29]. The improvements are assessed from the real-time operation in comparison with the two-variable FLC system. The sample period and the numerical integration method selected ensure numerical stability and accuracy of the MATLAB^{TM}-Simulink based simulations used.

This research is motivated by the need to tackle the problems in controlling of the levels in distillation and carbonisation columns for synthetic soda ash production where the empirically designed PLC-based classic PI control causes oscillations both in the levels and the controls which results in fast wearing out of the expensive actuators.

The paper is organized as follows. Section 2 presents previous investigation and problem formulation. The description of the plant, the design of a model-free FLC for the control of the two coupled levels, the experiments from the real-time plant control and the GAs derivation and the validation of the transfer matrix-based TSK plant model are explained in Section 3. An optimal in structure FLS is developed in Section 4. The approximation of the SAFLC by a parallel distributed compensation (PDC) and the study of the SAFLC system stability via Lyapunov – linear matrix inequalities (LMIs) approach comprise Section 5. Section 6 summarizes the main results and outlines the future research.

2. Previous Investigation and Problem Formulation.

The basic idea for an SAFLC is developed in [2,9,10,27] for single-input single-output (SISO) plants – the air temperature in a dryer [9,27], and different main controllers – linear, FLC, PDC. An FLS from a second control level continuously adjusts the main controllers' gains and ScFs to keep different performance indicators $\mathbf{\Pi}_i$ within their defined terms "Norm". The performance measures $\mathbf{\Pi}_i$ are easily estimated on-line from current and past measurements. An example for an SAFLC system with a main controller and an FLS is shown in Figure 1.

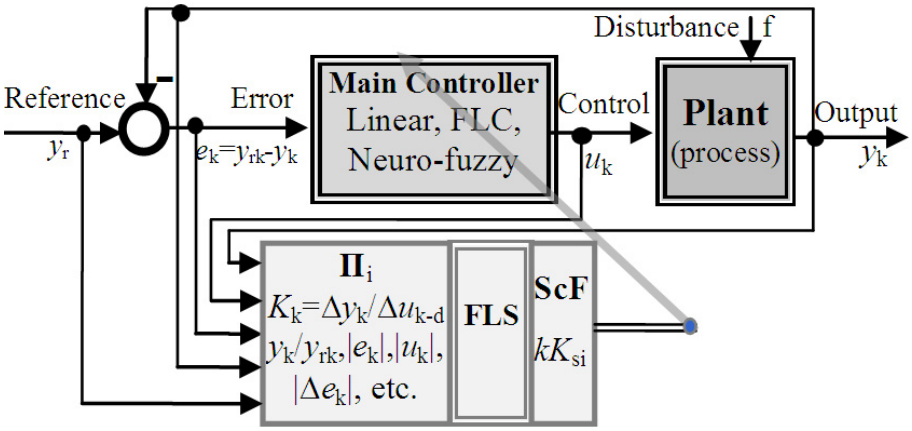

FIGURE 1. Block diagram of an SAFLC system

The performance is assessed by the current moment t_k estimate of the plant gain K_k accounting for the plant time delay $\tau = \mathrm{d}.\Delta t$, the over/undershoot y_k/y_{rk}, the absolute error $|e_k|$, the change of error $|\Delta e_k|$, the control $|u_k|$, etc., where Δt is the sample period and y_r is the reference of the output y. The scaled by kK_s FLS outputs auto-tune on-line the ScFs or the gains of the main controller. The FLS structure design is not based on systematic approach. The transfer function based TSK plant model needed for the design of a PDC is derived from plant step responses empirically [9,27] and is not validated. A SISO TSK GAs parameter optimization, a simulations-based GAs approximation of the more complicated SISO SAFLS to a simpler SISO PDC, a SISO PDC validation from real time control data and a TSK-PDC system stability analysis are first suggested in [27].

The problem in the present paper is to develop a systematic approach for the design of model-free SAFLCs for nonlinear MIMO plants using the example of the control of coupled liquid levels – a nonlinear two-variable plant without self-regulation and a reliable model which cannot be controlled by classic means. The performance of the SAFLC system is assessed from real-time control in comparison with a two-variable FLC system.

The tasks to be solved comprise the steps of the suggested approach, presented in the next sections:

(a) Design a model-free main FLC for a MIMO plant, and derive and validate a transfer matrix based TSK plant model from expert and experimentation real-time plant control data;

(b) Design a MIMO FLS of optimal structure for adaptation of the ScFs of the main FLC;

(c) Approximate the MIMO SAFLC (FLC-FLS) by a simple PDC to satisfy the requirements for PLC implementations [30] and validate the PDC from experimental data;

(d) Validate the MIMO SAFLC system stability.

The TSK plant modelling and the SAFLC approximation by a PDC use the GAs optimization technique and real-time control data. The GAs are selected as a proper derivative-free stochastic method for multi-criteria optimization with respect to a great number of parameters. A parallel search of a global minimum of multimodal and nonlinear cost functions under different restrictions defined on data from simulation or experiments is ensured. The GAs optimization is difficult to apply on-line as it influences the real plant operation. Besides, it is slow since many experiments are required. The accuracy is affected by various disturbances from the industrial environment and the restrictions related with the system stability and the bounds on parameters and signals. The off-line

GAs optimization is based on an accepted fitness function evaluated via simulations using an accurate plant model and a representative sample of processed experimentation data.

Level control is important for ensuring of energy and material balance in many installations [1,27] and is also difficult due to the specific plant characteristics such as oscillations, lack of self-regulation, MIMO character, and nonlinearity. SISO controllers for level are developed in [31-33] – a GAs parameter optimized linear PID in [32] and an FLC in [31], both tested via simulations, and a GAs parameter optimized FLC using a multi-objective fitness function in [33] for real-time control. In [34] a TSK-based two-variable linear controller and a PDC of local two-variable linear controllers for coupled levels are designed from requirements for decoupling and compared in real-time control.

The present design approach is demonstrated using the described in [34] laboratory coupled-tank system, the empirically designed two-variable model-free Mamdani PI-FLC, here used as a main MIMO controller, and the derived transfer matrix-based TSK plant model via GAs parameter optimization and validated in the real-time plant FLC control.

The novelty concludes in the suggested systematic approach for a model-free design of a MIMO SAFLC system ensuring stability and good performance via a PLC feasible controller. It includes development of an optimal in structure MIMO FLS based on system performance sensitivity analysis, GAs approximation of the developed SAFLC to a computationally economic MIMO PDC and its validation from real-time control data to be performed by industrial PLCs [30], MIMO SAFLC system stability validation using a TSK-PDC system representation and a modification of the Lyapunov stability conditions and their corresponding LMIs [35].

3. **Plant Description, MIMO FLC Design and TSK Modelling.** In this section step (a) of the systematic SAFLC design approach is presented – the description of the plant, the empirical model-free design of a two-variable PI-FLC, the FLC system reference step responses from real-time coupled levels control and the derivation from them of a MIMO TSK plant model [34].

The plant is a laboratory-scale two-tank level control system, shown in Figure 2 [34]. It consists of two identical tanks, each equipped with a pump, a pump amplifier and a pressure cell level sensor with a transmitter. Pump 1 at the bottom of the collector tank pumps up liquid to the top of Tank 1 and then down to fill it. Pump 2 at the bottom of

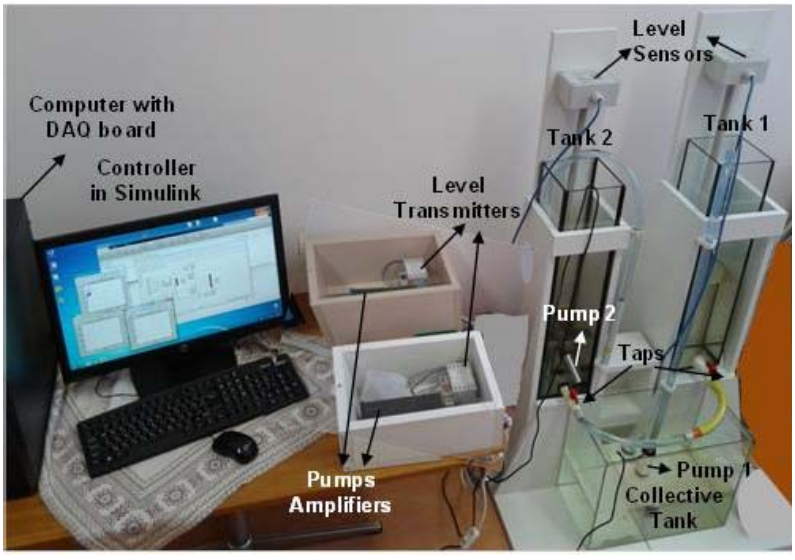

FIGURE 2. Laboratory-scale coupled tanks system

Tank 2 empties it pumping liquid up to the tank top and then out into the collector tank. A piping connects the two tanks via their taps at the bottom. The plant is a nonlinear two-variable system with output controlled variables (H_1, H_2) and input control (U_1, U_2). In each linear range it can be presented by a transfer matrix:

$$P(s) = \begin{bmatrix} P_{11}(s) & P_{12}(s) \\ P_{21}(s) & P_{22}(s) \end{bmatrix}, \tag{1}$$

where $P_{ij}(s)$ is the transfer function from plant input U_j to output y_i $(y_i = H_i)$.

The plant output y_i is a sum of the outputs from the main and the cross channels:

$$y_i(s) = y_{ii}(s) + y_{ij}(s), \quad i, j = 1, 2, \quad y_{ij}(s) = P_{ij}(s)U_j(s),$$

i.e., $H_1 = H_{11} + H_{12} = P_{11}(s)U_1 + P_{12}(s)U_2$, $H_2 = H_{21} + H_{22} = P_{21}(s)U_1 + P_{22}(s)U_2$.

The main channels $P_{ii}(s)$ (the faster and with the higher gains) are output H_1-input U_1 with output component y_{11} and H_2-U_2 with output component y_{22} $(y_{ii} = H_{ii})$. The cross channels are H_1-U_2 and H_2-U_1 with output components y_{12} and y_{21}. The gains in $P_{11}(s)$ and $P_{21}(s)$ are positive as an increase in U_1 leads to an increase in H_1 and H_2. The gains in $P_{22}(s)$ and $P_{12}(s)$ are negative because an increase in U_2 causes a decrease in H_2 and H_1. The plant is without self-regulation or ill-defined since a step change in U_1 causes an overflow in both tanks and a step change in U_2 empties them. The pumps operate with thresholds and in pumping up liquid in or out of the tanks they have to overcome the pressure of an 80 (cm) tubing full of liquid. It makes the derivation of a simple and also accurate enough nonlinear plant model difficult. The design of a controller using classical approaches is impossible.

A data acquisition (DAQ) board with analog-to-digital converter (ADC) and digital-to-analog converter (DAC) is the plant-computer interface. The corresponding measured level by the sensor is passed to the level transmitter for conditioning and then to the ADC. A Simulink model in MATLAB™ that performs the real-time controller reads via an Analog input driver the ADC binary code and converts it to level, filters the measurement noise, generates the reference signals, computes the necessary control, and graphically represents signals. The computed control U_i is limited within $[0, 10]$ (V) and passed via the Analog output driver in the Simulink model to the DAC and from there to the pump amplifier of the corresponding pump. The ranges for H_i are $[10, 40]$ (cm). The insensitivity thresholds for Pump 1 and Pump 2 are 3 (V) and 2 (V) respectively.

The main controller of the plant is the suggested in [34] a two-variable FLC. It consists of two identical in structure model-free Mamdani PI-FLCs – PI-FLC1 for the control of Level 1, shown in Figure 3, and PI-FLC2 for the control of Level 2. The fuzzy units (FUs) are identical each with two inputs – the normalized in the range $[-1, 1]$ errors in the main channel e_{in} and in the cross channel e_{jnc} $(i \neq j;\ i, j = 1 \div 2)$, standard triangle and trapezoidal MFs and hard rules. The post-processing is also identical – PI algorithms with empirically tuned parameters $K_{pi} = 5$ and K_{Ii}=5/100 to ensure operation with U_i in the range $[0, 10]$ (V) for references H_{ri} in the range $[10, 40]$ (cm). The ScFs are computed for the maximal expected error $\Delta e = \pm 10$ cm – $K_{e1} = 0.1$ and $K_{e2} = -0.1$. The negative sign is used to inverse the logic of the FU to reflect the negative gains of the plant with respect to input U_2. The constant $U_i(0)$ compensates the pump threshold. The ScFs are empirically tuned $-K2_{e2} = -0.2$ in FLC1 (the minus compensates the negative gain K_{e2} in FLC2) and $K2_{e1} = 1$ in FLC2.

The experimental step responses of the two levels H_{iex} and the corresponding controls U_{iex} of the FLC closed loop system to different references from the real-time plant control are presented in Figure 4 and Figure 5. The data (H_{iex}, U_{iex}) are used for the TSK plant modeling.

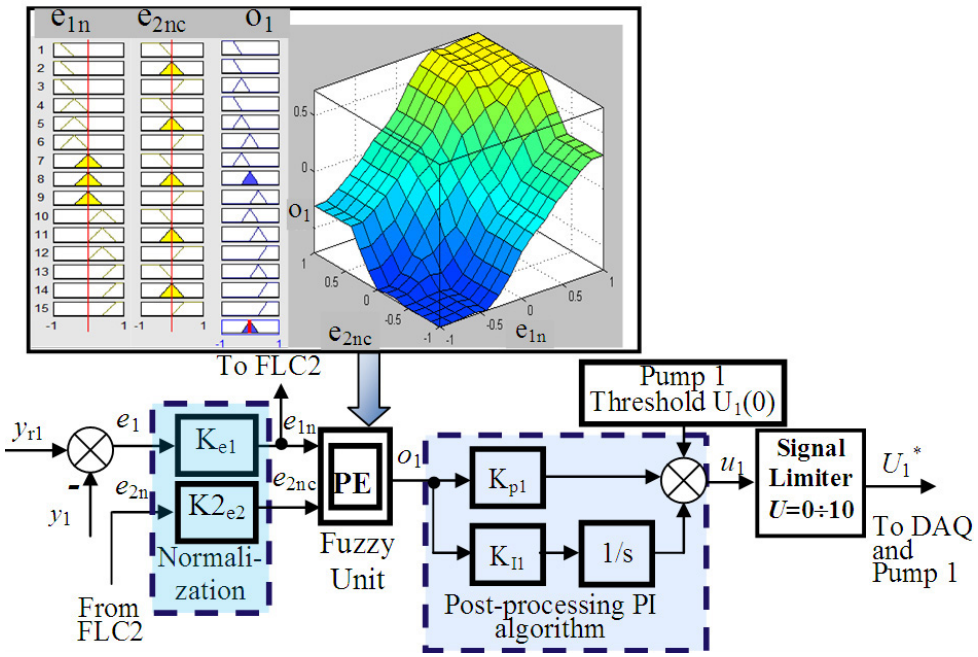

FIGURE 3. Block diagram of PI-FLC1 for Level 1 of the two-variable PI-FLC

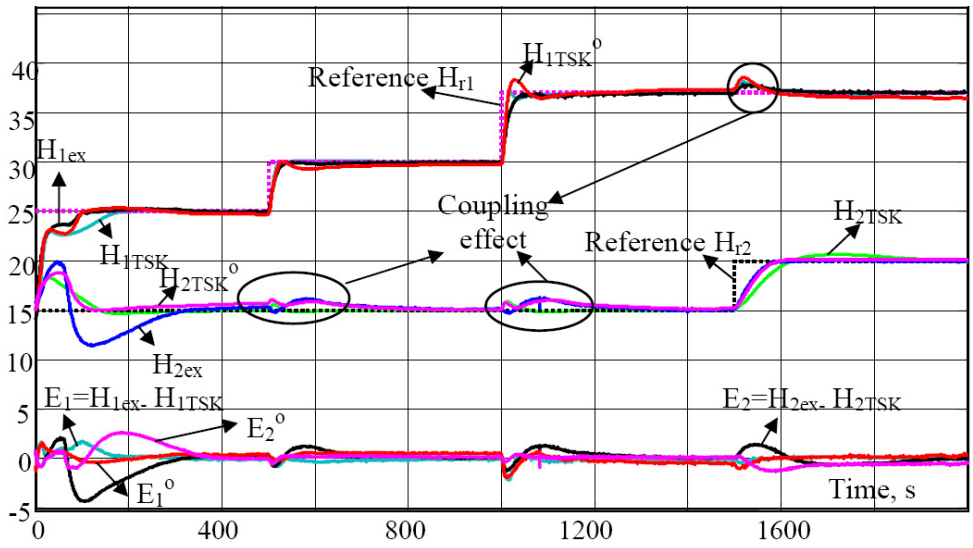

FIGURE 4. Step responses of levels H_{1ex} and H_{2ex} from two-variable FLC real-time control and TSK plant modelling

The TSK plant model assumes a two-variable linear model with transfer matrix representation for each local linearization zone. Two Sugeno models, designed by experts, define three linearization operation ranges (zones) – Sugeno 1 for Level 1 $y_1 \in [0, 60]$ (cm), shown in Figure 6, and Sugeno 2 for Level 2 identical to Sugeno 1 but with $y_2 \in [0, 30]$ (cm). The input of each Sugeno model is the corresponding current level $y_1 = H_1$ or $y_2 = H_2$ and the three outputs are described by three MFs singletons. The outputs yield the current degrees of belonging μ_k $(k = 1 \div 3)$ of y_i to the defined linearization zones. Without loss of generality, the model structure can easily be extended for "n" linearization zones and "m" main channels.

The local two-variable plant can be represented by a main and a cross channel determined by experts each consisting of two time-lags in series. One of the time lags is assumed

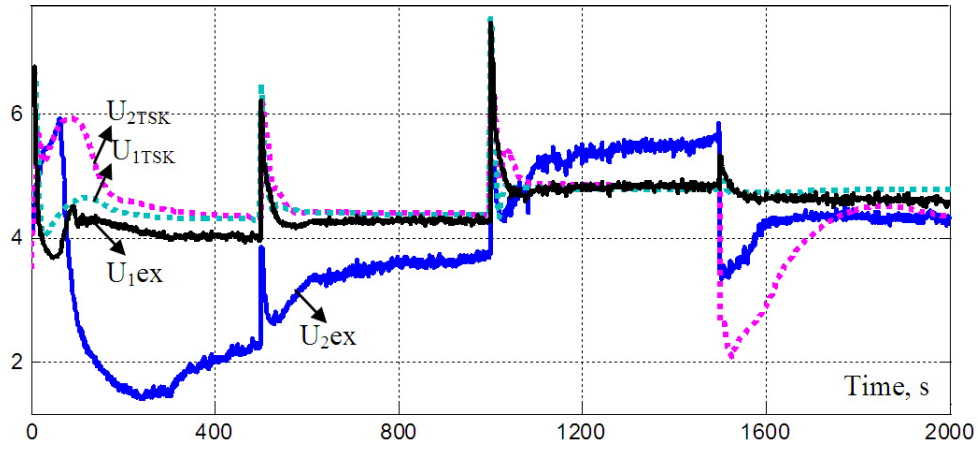

FIGURE 5. Control actions in FLC real-time control and in TSK plant modeling

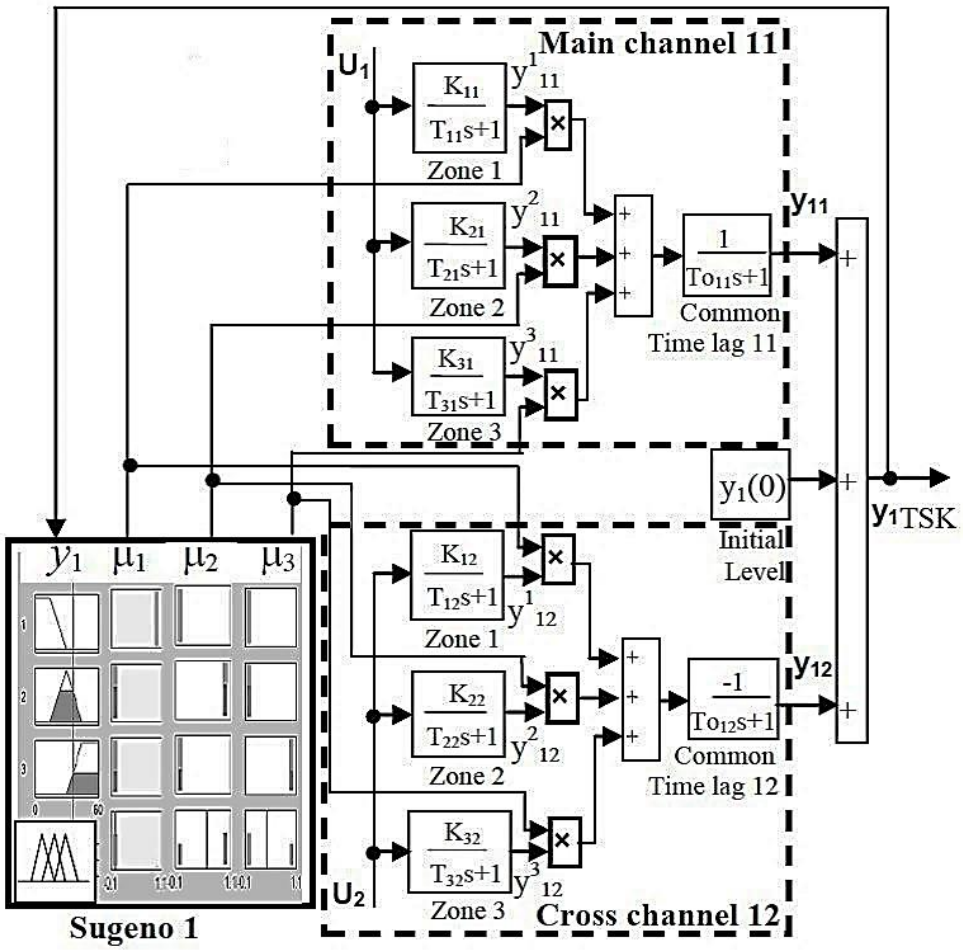

FIGURE 6. TSK plant model for output level 1 $y_{1\mathrm{TSK}} = H_{1\mathrm{TSK}}$

common for all zones and with a fixed time-constant T_{oij}. Here $T_{o11} = T_{o21} = 10$ (s) for the faster channels with input U_1 to the more powerful Pump 1 and $T_{o12} = T_{o22} = 40$ (s) for the channels with input U_2. The initial levels are $y_1(0) = y_2(0) = 15$ (cm) as shown in Figure 4.

The TSK plant model parameters $\mathbf{q}_{\mathrm{TSK}}$ are the gains K_{ij}^k and the time-constants T_{ij}^k of the time-lags in all zones in the four main and cross channels with outputs y_{11}, y_{12}, y_{22},

y_{21}:

$$\mathbf{q}_{\mathrm{TSK}} = \begin{bmatrix} K_{11}^1 & K_{11}^2 & K_{11}^3 & T_{11}^1 & T_{11}^2 & T_{11}^3 & K_{12}^1 & K_{12}^2 & K_{12}^3 & T_{12}^1 & T_{12}^2 & T_{12}^2 \\ K_{21}^1 & K_{21}^2 & K_{21}^3 & T_{21}^1 & T_{21}^2 & T_{21}^3 & K_{22}^1 & K_{22}^2 & K_{22}^3 & T_{22}^1 & T_{22}^2 & T_{22}^3 \end{bmatrix}.$$

They are computed using the GAs minimization of the sum of the relative integral squared modeling errors in the two main channels:

$$\mathbf{F}_{\mathrm{TSK}} = \int \sum_{i=1}^{2} \left\{ \left[H_{i\mathrm{TSK}}(t) - H_{iex}(t) \right] / H_{iex}(t) \right\}^2 dt \to \underbrace{\mathbf{min}}_{\mathbf{q}_{\mathrm{TSK}}}. \tag{2}$$

The TSK plant model inputs are $U_i = U_{iex}$, $y_i = H_{iex}$ in Figure 4 and Figure 5 from the two-variable PI-FLC real-time plant control. Its outputs $y_{i\mathrm{TSK}}(t) = H_{i\mathrm{TSK}}(t)$ are compared with the real plant outputs $H_{iex}(t)$. In order to model successfully the plant nonlinearity, the closed loop FLC system is subjected to a variety of reference changes so that the data (U_{iex}, H_{iex}) are rich in magnitudes and frequencies. The data are pre-processed omitting the uninformative steady state values thus reducing the sample in size. Here the values for (U_{iex}, H_{iex}) considered in the GAs optimization of (2) are selected from the time ranges $t =$ 0-800; 1000-1300; 1500-1700. The computed optimal TSK plant model parameters ($\mathbf{F}_{\mathrm{TSKmin}} = 3.92$) are:

$$\mathbf{q}_{\mathrm{TSK}} = \begin{bmatrix} 1.00 & 3.6 & 6.0 & 5.4 & 4.60 & 6.30 & 0.85 & 0.18 & 0.08 & 0.95 & 1.86 & 0.95 \\ 0.15 & 0.6 & 1.7 & 0.5 & 0.98 & 14.1 & 0.33 & 0.60 & 0.18 & 48.0 & 5.20 & 1.30 \end{bmatrix}.$$

The GAs parameters are 20 generations, a single-point crossover, mutation in one bit and a roulette type selection. The simulated TSK plant model outputs $H_{i\mathrm{TSK}}^{\mathrm{o}}(t)$ for inputs (U_{iex}, H_{iex}) and $t = 0 \div 2000$ are shown in Figure 4. The modeling error $E_i^{\mathrm{o}} = H_{iex} - H_{i\mathrm{TSK}}^{\mathrm{o}}$ is small which shows that the TSK plant model is accurate. This TSK model is used in simulations of the closed loop system which step responses $H_{i\mathrm{TSK}}(t)$, also presented in Figure 4, differ a little from $H_{i\mathrm{TSK}}^{\mathrm{o}}(t)$ since the inputs to Sugeno 1 and Sugeno 2 are already the TSK plant model outputs. The modeling error remains small. Since all experimental values (U_{iex}, H_{iex}) are used in evaluating the TSK model accuracy while only a selection of them is included in the TSK modeling, it can be concluded that the model is successfully validated. Further validation is carried out with a new type of control from the designed SAFLC in Section 5.

4. **Design of a Two-Variable Fuzzy Logic Supervisor.** The empirically tuned MIMO PI-FLC ensures system stability but some of the system performance indices, estimated from the FLC system step responses, can be improved by on-line adaptation of the FLC ScFs from an upper control level FLS. This section presents step (b) from the systematic SAFLC design approach – design of a second level MIMO FLS of optimal structure to guarantee its efficiency based on system performance sensitivity analysis using TSK plant model-based simulations. The FLC system step responses in Figure 4 and Figure 5 show that the settling time t_s and the coupling between the channels ($H_2(t)$ in step responses 2 and 3 and $H_1(t)$ in step response 4) can be reduced by introducing of a proper MIMO FLS. The energy efficiency of the control can also be increased by decreasing the controls magnitudes and oscillations.

The FLS is built using simple single-input single-output (SISO) FUs which can be easily designed out of empirical knowledge, satisfying a desired criterion with respect to a specific performance indicator via adapting some ScF. With the use of multiple FUs the FLS structure becomes complex and needs a careful design in order to ensure the most efficient fulfillment of the nonlinear multi-criteria system performance optimization.

Inputs to the FUs are the performance indicators $\mathbf{\Pi}_i$ to be improved. They are computed from on-line current and past measurements. Outputs of the FUs are correction gains and their functional relationship with the adapted ScFs. Here the FLC system performance indicators to be improved via FLS are related with the plant output and the control specifications. For each performance indicator $\mathbf{\Pi}_i$ the proper ScF_j with the most efficient influence on $\mathbf{\Pi}_i$ is determined. This shapes the FLS structure of a number of SISO FUs with defined inputs and outputs. For this purpose the FLC system relative sensitivity $S_{\mathbf{\Pi}_i} = \frac{\Delta\mathbf{\Pi}_i}{\mathbf{\Pi}_i^{\mathrm{o}}} \Big/ \frac{\Delta q_{\mathrm{ScF}_j}}{\Delta q^{\mathrm{o}}_{\mathrm{ScF}_j}}$ is studied via simulations, where $\Delta\mathbf{\Pi}_i = \mathbf{\Pi}_i - \mathbf{\Pi}_i^{\mathrm{o}}$ and $\Delta q_{\mathrm{ScF}_j} = q_{\mathrm{ScF}_j} - q^{\mathrm{o}}_{\mathrm{ScF}_j}$ are the variations of the performance indicator and of the ScF respectively from their nominal (initially tuned) values, denoted by 'o'. Here it is assumed that $\Delta q_{\mathrm{ScF}_j} \Big/ q^{\mathrm{o}}_{\mathrm{ScF}_j} = 10\%$. The relative sensitivity is a measure of the relative change in $\mathbf{\Pi}_i$ at a relative change of a ScF – here $\Delta\mathbf{\Pi}_i/\mathbf{\Pi}_i^{\mathrm{o}} = S_{\mathbf{\Pi}_i}.0,1$. The FLC system ScFs are $\mathbf{q}_{\mathrm{ScFs}} = [K_{e1}, K2_{e2}, K_{p1}, K_{I1}, K_{e2}, K2_{e1}, K_{p2}, K_{I2}]$ with nominal values from empirical tuning $\mathbf{q}^{\mathrm{o}}_{\mathrm{ScFs}} = [K^{\mathrm{o}}_{e1} = 0.1, K2^{\mathrm{o}}_{e2} = -0.2, K^{\mathrm{o}}_{p1} = 5, K^{\mathrm{o}}_{I1} = 5/100, K^{\mathrm{o}}_{e2} = -0.1, K2^{\mathrm{o}}_{e1} = 1, K^{\mathrm{o}}_{p2} = 5, K^{\mathrm{o}}_{I2} = 5/100]$. The performance indicators accounted for are $\mathbf{\Pi}_{1,2} = y_i/y_{ri}$, $\mathbf{\Pi}_{3,4} = |e_{in}|$, $\mathbf{\Pi}_{5,6} = |o_{in}|$.

The most effective ScF_j for the adaptation of $\mathbf{\Pi}_i$ is selected from the relatively high, smooth and uniform in time $S_{\mathbf{\Pi}_i}(t)$ for all system step responses of the two outputs. The effects of ScFs' variations have to be symmetrical for the two output channels, e.g., an increase in K_{p1} results in a decrease mainly in $\mathbf{\Pi}_1$, and an increase in K_{p2} leads to a decrease mainly in $\mathbf{\Pi}_2$. The adaptation of $K2_{ej}$ can reduce y_i/y_{ri} in the step responses and hence can decrease the cross-channel coupling.

The study of the FLC system sensitivity $S_{\mathbf{\Pi}_i}(t)$ determines a symmetrical optimal structure of the two-variable FLS (symmetrical structures support MIMO systems stability). It consists of FLS1 for auto-tuning of PI-FLC1, shown in Figure 7, and an identical in structure FLS2 for auto-tuning of PI-FLC2. Each FLSi has two FUs to fulfill the requirements to two performance-based criteria:

- FU_1 with input $y_i/y_{ri} \in [0,2]$ and output $kK2_{ej}$ that scales $K2_{ej}$ in order to reduce the cross-channels impact;

- FU_2 with input $|o_i| \in [0,1]$ and output kK_{pIi} that scales both K_{pi} and K_{Ii}. This is a fast and direct way to influence the control action and reduce t_s, the overshoot σ and the control effort, but may cause control oscillations due to the continuous adaptation.

The term 'Norm' for y_i/y_{ri} is about 1 and for $|o_i|$ is about 0.5. The MFs for the FUs inputs y_i/y_{ri} and $|o_i|$ can be defined in a common universe of discourse $[0,2]$ – the larger of the two ranges. The MFs for the FUs outputs $kK2_j$ and kK_{pIi} can be defined in the range $[0,2]$ to allow an increase and a decrease of the corresponding ScFs, i.e., $K2_{ej}$ and (K_{pi}, K_{Ii}) can be scaled by greater and smaller than 1 gains $kK2_{ej}$ and kK_{pIi} respectively. The MFs are standard, small in number and symmetrical with respect to the term 'Norm'. The fuzzy rules for FU_1 and FU_2 can be identical and of the type as below:

IF $\mathbf{\Pi}_i$ is 'Above Norm' **THEN** Scaling gain kK is 'Small' (reduce control), etc.

Thus, a single FU is designed and used for FU_1 and FU_2. For additional tuning each FU is provided with an output tuning parameter $\mathrm{ScF}_{\mathrm{FLS}i} = [K_{\mathrm{FU}1i} \quad K_{\mathrm{FU}2i}]$ to conform signals. The input y_i/y_{ri} to FU_1 takes values in the whole range $[0,2]$. So, its output $kK2_{ej}$ can cover the whole output range $[0,2]$. In order to prevent signals beyond the normalization range $[-1,1]$ $K_{\mathrm{FU}11} = K_{\mathrm{FU}12} = 0.5$ in FLS1 and FLS2 respectively. The input $|o_i|$ to FU_2 takes values in the range $[0,1]$ – half of the range, defined for the input of FU, so kK_{pIi} covers half of the FU output range $[0,2]$. Therefore, $K_{\mathrm{FU}21} = K_{\mathrm{FU}22} = 2$ in FLS1 and FLS2 to enable adaptive change of K_{pi} and K_{Ii} above and below their initially

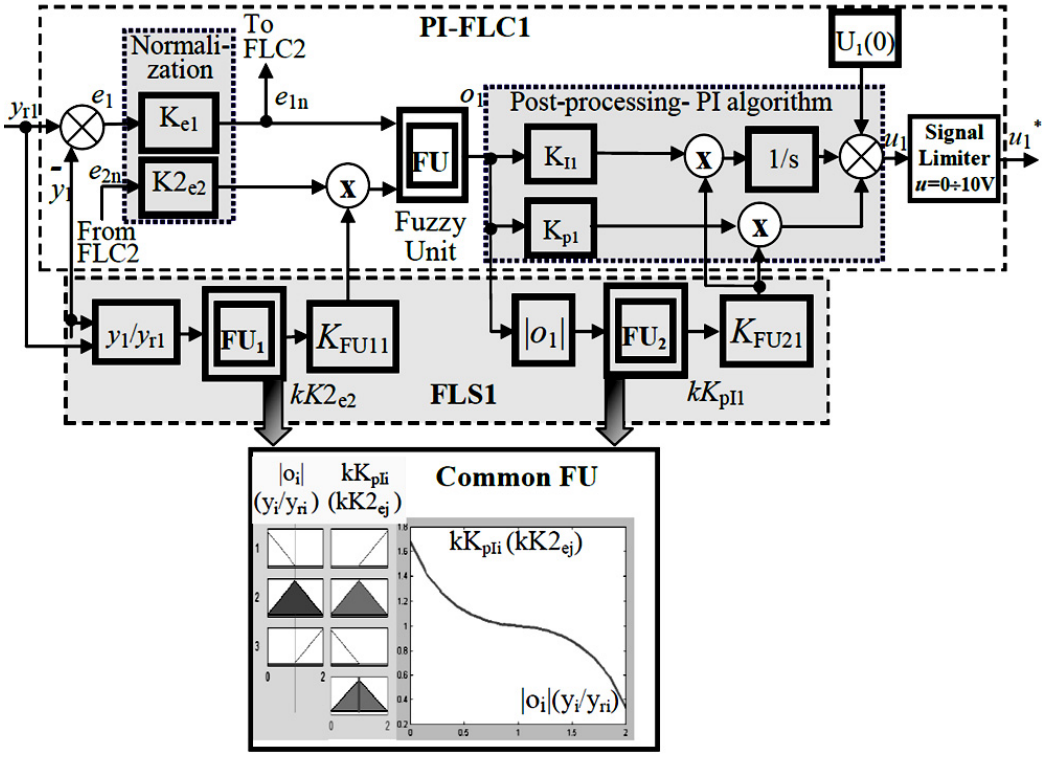

FIGURE 7. Block diagram of PI-FLC1-FLS1 for main channel 1 – FU = $FU_1 = FU_2$

tuned values. The FUs tuning parameters and output MFs ranges are expert defined to preserve the FLC system stability and also to ensure the performance norms for all expected changes in the plant.

The experimental step responses with respect to the tanks levels and the controls from the real-time control in the SAFLC system are depicted in Figure 8 and Figure 9 respectively. The step responses from simulation of the SAFLC system with the developed TSK plant model are also shown for comparison and for the purpose of TSK plant model validation. The experimental and the simulation results for levels and control actions are close. This confirms the accuracy of the TSK plant model for arbitrary inputs in the ranges and justifies its further use for validating the adaptive FLC system stability. The reference step changes cover the operation range and allow estimating the influence of the nonlinearity on the performance indicators. The level and the control reference step responses of the FLC system from real-time operation are overlaid on the same figures to facilitate the assessment of the performance improvements due to the FLS. The first step responses are provoked both by a reference change and a different from equilibrium initial condition for the control. Therefore, they are not accounted for in the performance analysis.

The FLS reduces the settling time t_s from 2 to 5 times for H_1 and from 1.5 to 3 times for H_2. The cross-channels impact is also reduced in magnitude and duration 3 times for H_1 in the last step response and from 1.5 to 3 times for H_2 in the second and the third step responses. The control actions at the beginning of the reference changes are greater in magnitude to assist the faster response and then they settle fast which explains the reduced t_s. The FLS changes significantly U_2 and insignificantly U_1.

The adaptation is illustrated in Figure 10(a) via the changes of the scaled by $K_{\mathrm{FU}ij}$ outputs of the FUs in the FLS – $kK2_{e2}$ and kK_{p1} for the channel with control U_1 and $kK2_{e1}$ and kK_{p2} for the channel with control U_2. The adapted $kK2_{ei}$ and kK_{pi} in a

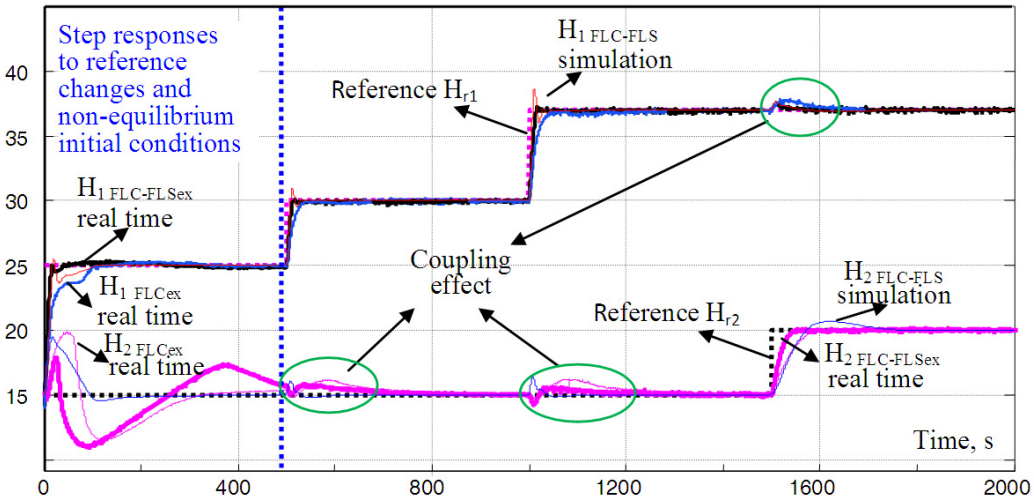

FIGURE 8. Step responses from real-time PI-FLC control with FLS $H_{i\text{FLC-FLSex}}$ and without FLS $H_{i\text{FLCex}}$ and from FLC-FLS system simulation $H_{i\text{FLC-FLS}}$

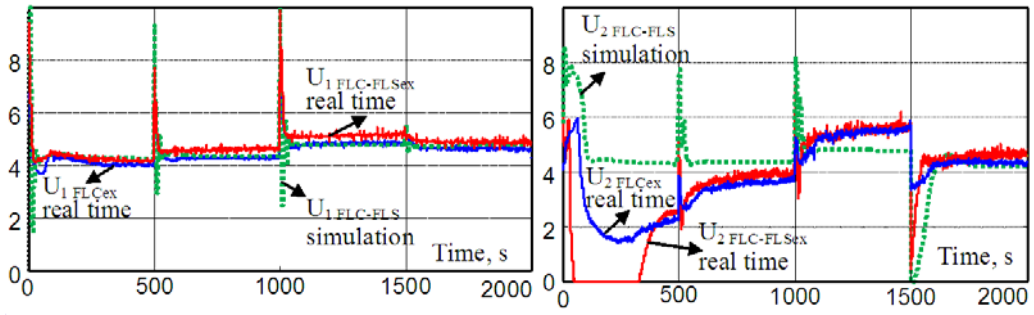

FIGURE 9. Control actions from real-time control with two-variable PI-FLC with FLS $U_{i\text{FLC-FLSex}}$ and without FLS $U_{i\text{FLCex}}$ and from FLC-FLS system simulation $U_{i\text{FLC-FLS}}$

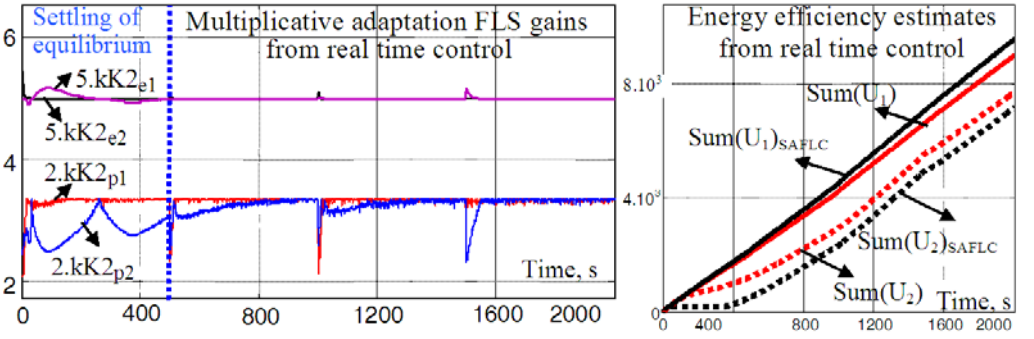

(a) (b)

FIGURE 10. Adaptation of FLS outputs (a) and energy efficiency estimates (b)

multiplicative way modify the ScFs $K2_{ei}$ and K_{pj} of the two main FLCs according to Figure 7. The ScF K_{p2} varies with greater magnitudes and duration. The adaptation starts for any change in the system errors caused by changes in references, disturbances, plant properties, etc. It settles within the settling time of the corresponding step response from Figure 8, which shows a good convergence rate. The final FLS outputs for each step response return to their initial values – an evidence for bringing of the system performance

indicators to their "norm" term. Estimates for energy efficiency are presented in Figure 10(b). The accumulated for the time of the experiments control action $\mathrm{Sum}(U_i)$ is accepted as a measure for the energy consumed in the levels control. The adaptation, introduced by the FLS, reduces the energy consumption mainly with respect to U_2.

5. **Validation of the Stability of the Two-Variable SAFLC System.** The stability analysis of the designed closed loop system is important because the system is nonlinear, multivariable and with variable parameters. The empirical expert knowledge used to design the main model-free Mamdani PI-FLC and the FLS ensures system stability under restrictions on signals and plant changes. Therefore, the experimental study of the designed two-variable FLC and SAFLC systems for some reference changes shows stable step responses (Figure 4, Figure 8). However, the stability of the designed two-variable AFLC system has to be validated in general, accounting for all possible operation modes, conditions and points in the range of operation of the equipment and of the processes.

Here steps (c) and (d) of the systematic SAFLC design approach are presented – the designed SAFLC is equivalently represented by a PDC in order to study the two-variable SAFLC system stability, based on the derived in [27,35] TSK-PDC Lyapunov-LMIs stability conditions. A PDC approximation of the SAFLC is selected on the grounds that each nonlinear dynamic system can be described by a TSK model of different complexity and for each TSK plant model there can always be designed a corresponding PDC [35]. Besides, the PDC is simpler in structure with reduced number of FUs and standard local linear controllers and requires less computational resources which make it suitable for industrial PLC implementation in real-time control. The PDC structure is suggested on the basis of the already derived TSK plant model. It consists of the same FUs – Sugeno 1 for H_1 and Sugeno 2 for H_2, to define and recognize the same three linearization zones as in the transfer matrix-based TSK plant model. For each linearization zone the local two-variable plant is controlled by a corresponding two-variable linear controller with transfer matrix:

$$C(s) = \begin{bmatrix} C_{11}(s) & C_{12}(s) \\ C_{21}(s) & C_{22}(s) \end{bmatrix}, \tag{3}$$

where the main controllers are linear PI with transfer functions $C_{ii}(s) = K_{pii} + K_{Iii}/s$.

The cross controllers approximate decoupling controllers $C_{ji}(s) = -P_{ji}(s)C_{ii}(s)/P_{jj}(s)$ in the local linear two-variable system. The local plant transfer functions in the main $P_{jj}(s)$ and in the cross-channel $P_{ji}(s)$ are time-lags with close time constants. Their denominators can be cancelled yielding PI cross controllers. Each control action is computed as a sum of two components – from the main channel controller U_{ii} and from the cross controller $U_{ij} - U_i = U_{ii} + U_{ij} = C_{ii}(s)e_i + C_{ij}(s)e_j$. So, the PDC consists of two identical components – one for U_1, shown in Figure 11, and one for U_2. The subscripts '1'-'3' of the PI controllers denote the linearization zones. The parameters of the two-variable controllers in the three zones are $\mathbf{q}_{\mathrm{PDC}} = [\mathbf{q}^1_{\mathrm{PDC}} \quad \mathbf{q}^2_{\mathrm{PDC}} \quad \mathbf{q}^3_{\mathrm{PDC}}]$, where $\mathbf{q}^k_{\mathrm{PDC}} = \begin{bmatrix} K^k_{p11} & K^k_{I11} & K^k_{p12} & K^k_{I12} & K^k_{p21} & K^k_{I21} & K^k_{p22} & K^k_{I22} \end{bmatrix}$ are the parameters of the local controller in the kth linearization zone. They are computed using GAs minimization of the following fitness function:

$$\mathbf{F}_{\mathrm{PDC}} = \int \sum_{i=1}^{2} \left[U_{i\mathrm{PDC}}(t) - U_{i\text{FLC-FLS}}(t)\right]^2 / U_{i\text{FLC-FLS}}(t)^2 dt \to \underbrace{\mathbf{min}}_{\mathbf{q}_{\mathrm{PDC}}}, \tag{4}$$

where:

- $U_{i\text{FLC-FLS}}(t)$, $i = 1, 2$, are the processed control actions from the SAFLC (FLC-FLS) real-time control of the tanks levels in a closed loop system for different references, shown

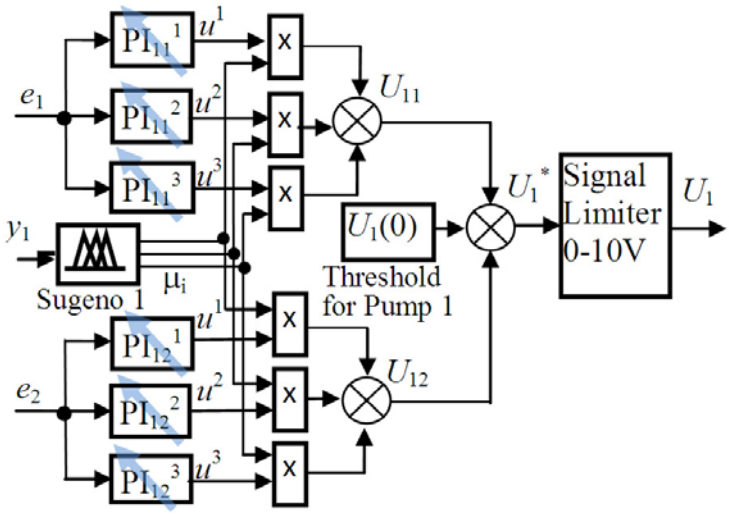

FIGURE 11. Block diagram of PDC for channel 1

in Figure 9. The processing concludes in elimination of uninformative settled values and smoothing via sliding average algorithm.

- $U_{i\mathrm{PDC}}(t)$ are the PDC outputs for the system errors from the real time control as inputs.

The optimal values computed for $\mathbf{q}_{\mathrm{PDC}}$ are:

$$\mathbf{q}_{\mathrm{PDC}}(K_{pij}, K_{Iij}) = \begin{bmatrix} \text{zone 1} & \text{zone 2} & \text{zone 3} \\ (0.582, 0.0238) & (0.747, 0.0099) & (0.923, 0.0097) \\ -(0.001, 0.0002) & -(0.006, 0.0002) & -(0.012, 0.0001) \\ (0.003, 0.0008) & (0.464, 0.0152) & (0.387, 0.0194) \\ -(0.017, 0.0133) & -(1.795, 0.0136) & -(0.353, 0.0109) \end{bmatrix}.$$

In Figure 12 the control actions $U_{i\text{FLC-FLSex}}(t)$ of the SAFLC from the real-time levels control and the control actions $U_{i\text{PDCex}}(t)$ of its PDC approximation are compared. The approximation error $E_i = U_{i\text{FLC-FLSex}} - U_{i\text{PDCex}}$ is small which gives grounds to test the PDC via simulations in a closed loop system with the TSK plant model. The step responses of the levels from the real-time control using the SAFLC and from the PDC system simulation are shown in Figure 13 and remain close. The control actions are also close.

The PDC is finally tested in real-time control of the tanks levels and the step responses $H_{i\text{PDCex}}(t)$, depicted in Figure 13, are close to the SAFLC system responses. This proves the functional equivalence between the more complex but easily designed SAFLC and the simpler for PLC implementation PDC. The first step responses are not accounted for because they start from non-equilibrium initial conditions for the controls.

The PDC validation is based on the levels real-time control with SAFLC and PDC for different in magnitude and time of application reference changes. The step responses $H_{i\text{PDCex}}(t)$ and $H_{i\text{FLC-FLSex}}(t)$ are shown in Figure 14 and remain close. Close are also the control actions $U_{i\text{PDCex}}(t)$ and $U_{i\text{FLC-FLSex}}(t)$. This demonstrates that the PDC is an accurate substitute of the SAFLC for all possible operation points in the defined ranges. The designed TSK plant model and PDC have learned well the nonlinearities and parameter changes in their GAs parameter optimization. This is due to the rich data used from the real-time levels control which contain the impact of disturbances related with the operation of the pumps, the appearance of air-pillows in the piping, mudding and foiling of taps, pipes, pumps filters, etc. So, the derived and validated TSK plant model and

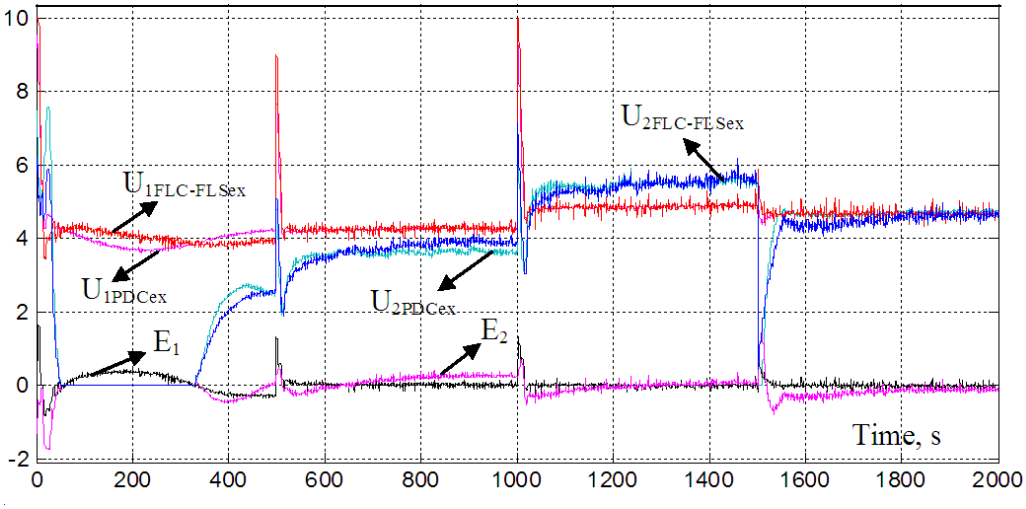

FIGURE 12. Control actions of PDC and SAFLC (FLC-FLS)

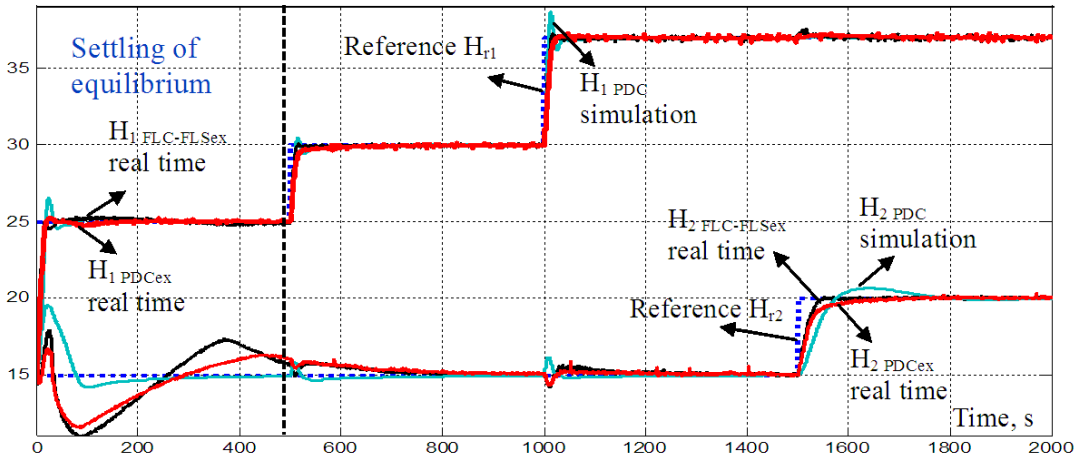

FIGURE 13. Levels step responses from simulation of PDC closed loop system and from real-time control with PDC and SAFLC (FLC-FLS)

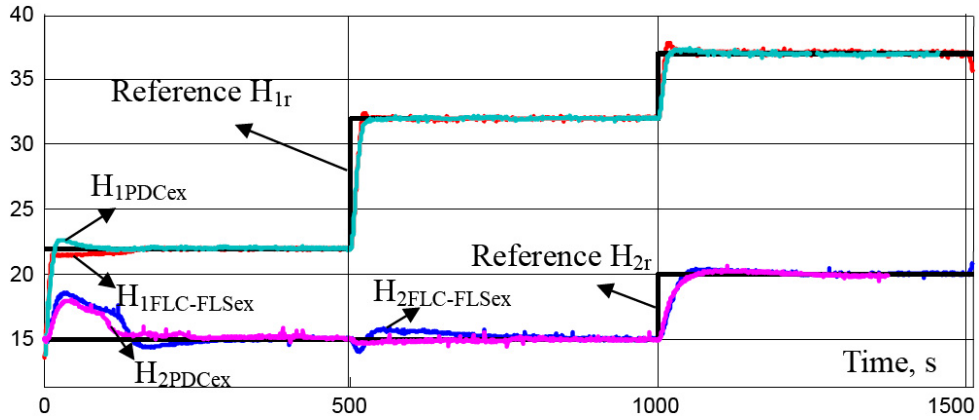

FIGURE 14. Levels step responses from real-time PDC and SAFLC for different references

PDC can be used to validate the SAFLC system stability in all operation and ambient conditions from the defined ranges for any step changes in reference and disturbances.

The transfer matrix-based TSK-PDC closed loop system is transformed into the standard form [27,35], described by the fuzzy rules:

$$\textbf{IF } y(t) \text{ is } M_k \textbf{ THEN } \left| \begin{array}{l} \dot{x}(t) = \boldsymbol{A}_k x(t) + \boldsymbol{B}_{\mathrm{k}} \dot{u}(t) \\ y(t) = \boldsymbol{C}_{\mathrm{k}} x(t) \end{array} \right. \tag{5}$$

$$\textbf{IF } y(t) \text{ is } M_k \textbf{ THEN } \left| \begin{array}{c} \dot{u}(t) = -\boldsymbol{F}_k x(t) + \boldsymbol{G}_k y_r \\ \text{or } \dot{u}(t) = K_{pk} \dot{e}(t) + K_{Ik} e(t) \end{array} \right. , \tag{6}$$

where the local controller in the kth linearization zone of the PDC is an incremental two-variable PI and the eliminated integrators are equivalently added to the local linear plant model. The vectors of the state variables $x(t)$, the control variables $u(t)$, the output variables $y(t)$, the references $y_r(t)$ and the errors $e(t)$ for the kth zone are:

$$x(t) = \left[x^1(t) \quad x^4(t) \quad x^7(t) \quad x^{10}(t) \right]^{\mathrm{T}}; \; x^p(t) = \left[\begin{array}{c} x_p(t) = y_{ij}(t) \\ x_{p+1}(t) = \dot{x}_p(t) \\ x_{p+2}(t) = \dot{x}_{p+1}(t) \end{array} \right];$$

$$u(t) = \left[u_1(t) \quad u_2(t) \right]^{\mathrm{T}}; \quad y(t) = \left[y_1(t) \quad y_2(t) \right]^{\mathrm{T}}; \; y_i(t) = y_{i1}(t) + y_{i2}(t);$$

$$y_r = \left[y_{r1} \quad y_{r2} \right]^{\mathrm{T}}; \; e(t) = \left[e_1(t) \quad e_2(t) \right]^{\mathrm{T}}, \; e_i(t) = y_{ri}(t) - y_i(t), \; i,j = 1,2; \; p = 1,4,7,10.$$

The model of the two-variable plant in (5) describes the dynamics of the main channels $y_{ii} - u_i$ ($p = 1$ for $i = 1$, $p = 10$ for $i = 2$) and the cross-channels ($p = 4$ for $i = 1$ and $j = 2$, $p = 7$ for $i = 2$, $j = 1$), each represented by a series connection of two time-lags and the integrator from the PI controller. For the kth linearization zone it is expressed by the matrices:

$$\mathbf{A}_k = \left[\begin{array}{cccc} \mathbf{A}_k^1 & 0 & 0 & 0 \\ 0 & \mathbf{A}_k^4 & 0 & 0 \\ 0 & 0 & \mathbf{A}_k^7 & 0 \\ 0 & 0 & 0 & \mathbf{A}_k^{10} \end{array} \right]_{12\times 12}, \; \mathbf{A}_k^p = \left[\begin{array}{ccc} 0 & 1 & 0 \\ 0 & 0 & 1 \\ 0 & -(1/T_oT)_k^p & -[(T_o+T)/T_oT]_k^p \end{array} \right]_{3\times 3},$$

$$\mathbf{B}_k = \left[\begin{array}{c} \mathbf{B}_k^1 \\ \mathbf{B}_k^4 \\ \mathbf{B}_k^7 \\ \mathbf{B}_k^{10} \end{array} \right]_{12\times 2}, \; \mathbf{B}_k^{1,7} = \left[\begin{array}{cc} 0 & 0 \\ 0 & 0 \\ (K/T_{\mathrm{o}}T)_k^{1,7} & 0 \end{array} \right]_{3\times 2}, \; \mathbf{B}_k^{4,10} = \left[\begin{array}{cc} 0 & 0 \\ 0 & 0 \\ 0 & (K/T_{\mathrm{o}}T)_k^{4,10} \end{array} \right]_{3\times 2},$$

$$\mathbf{C}_k = \left[\begin{array}{cccc} \mathbf{C}_k^1 & \mathbf{C}_k^4 & \mathbf{C}_k^7 & \mathbf{C}_k^{10} \end{array} \right]_{2\times 12}, \; \mathbf{C}_k^{1,4} = \left[\begin{array}{ccc} 1 & 0 & 0 \\ 0 & 0 & 0 \end{array} \right]_{2\times 3}, \; \mathbf{C}_k^{7,10} = \left[\begin{array}{ccc} 0 & 0 & 0 \\ 1 & 0 & 0 \end{array} \right]_{2\times 3}.$$

The local linear two-variable incremental PI main and cross controllers in the conclusions of (6) are described by the matrices:

$$\mathbf{F}_k = \left[\begin{array}{cccc} \mathbf{K}_k^{1,7} \big| \mathbf{O}_{2\times 1} & \mathbf{K}_k^{1,7} \big| \mathbf{O}_{2\times 1} & \mathbf{K}_k^{4,10} \big| \mathbf{O}_{2\times 1} & \mathbf{K}_k^{4,10} \big| \mathbf{O}_{2\times 1} \end{array} \right]_{2\times 12},$$

$$\mathbf{G}_k = \left[\begin{array}{cc} K_{I11k} & K_{I12k} \\ K_{I21k} & K_{I22k} \end{array} \right]_{2\times 2}, \; \mathbf{K}_k^{1,7} = \left[\begin{array}{cc} K_{I11k} & K_{p11k} \\ K_{I21k} & K_{p21k} \end{array} \right]_{2\times 2},$$

$$\mathbf{K}_k^{4,10} = \left[\begin{array}{cc} K_{I12k} & K_{p12k} \\ K_{I22k} & K_{p22k} \end{array} \right]_{2\times 2}, \; \mathbf{O}_{2\times 1} = \left[\begin{array}{c} 0 \\ 0 \end{array} \right].$$

The sufficient condition for systems (5) and (6) to have a globally asymptotically stable equilibrium state according to Lyapunov is the existence of a common for all local linear

systems positive determined matrix $\mathbf{P} > 0$ which satisfies the following matrix inequalities for m, $n = 1 \div k$, $n > m$ and activation degrees of the rules $h_m \cap h_n \neq \emptyset$ [27,35]:

$$\begin{cases} \mathbf{M}_{mm}^{\mathrm{T}}\mathbf{P} + \mathbf{P}\mathbf{M}_{mm} < 0 \\ 0.5\left(\mathbf{M}_{mn} + \mathbf{M}_{nm}\right)^{\mathrm{T}}\mathbf{P} + \mathbf{P}.0.5\left(\mathbf{M}_{mn} + \mathbf{M}_{nm}\right) \leq 0 \ . \\ \mathbf{M}_{mn} = \mathbf{A}_m - \mathbf{B}_m\mathbf{F}_n \end{cases} \tag{7}$$

The LMIs numerical method, developed for optimization problems from the linear programming under convex constraints [35], is used for solving (5). The constraint for $\mathbf{P} > \mathbf{0}$ is added to the linear inequalities (7). Because of the critical stability of the open loop system in presence of integrator in the controller more conservative conditions for the closed loop system stability are introduced by replacing the zero matrix $\mathbf{0}$ with a diagonal matrix with equal elements $o_{ij} > 0$ (here $o_{ij} = 20$).

The computed by the LMIs technique solution is:

$$\mathbf{P} = \begin{bmatrix} \mathbf{P}_{3\times3}^1 & \mathbf{O}_{3\times3} & \mathbf{O}_{3\times3} & \mathbf{O}_{3\times3} \\ \mathbf{O}_{3\times3} & \mathbf{P}_{3\times3}^2 & \mathbf{O}_{3\times3} & \mathbf{O}_{3\times3} \\ \mathbf{O}_{3\times3} & \mathbf{O}_{3\times3} & \mathbf{P}_{3\times3}^3 & \mathbf{O}_{3\times3} \\ \mathbf{O}_{3\times3} & \mathbf{O}_{3\times3} & \mathbf{O}_{3\times3} & \mathbf{P}_{3\times3}^4 \end{bmatrix},$$

where

$$\mathbf{P}_{3\times3}^1 = \begin{bmatrix} 0.6 & -0.003 & 0 \\ -0.003 & 0.613 & -0.001 \\ 0 & -0.001 & 0.613 \end{bmatrix}, \ \mathbf{P}_{3\times3}^2 = \begin{bmatrix} 0.613 & -0.001 & 0 \\ -0.001 & 0.613 & -0.001 \\ 0 & -0.001 & 0.614 \end{bmatrix},$$

$$\mathbf{P}_{3\times3}^3 = \begin{bmatrix} 0.613 & -0.001 & 0 \\ -0.001 & 0.613 & -0.001 \\ 0 & -0.001 & 0.613 \end{bmatrix}, \ \mathbf{P}_{3\times3}^4 = \begin{bmatrix} 0.613 & -0.001 & 0 \\ -0.001 & 0.613 & -0.001 \\ 0 & -0.001 & 0.613 \end{bmatrix}.$$

All minors of $\mathbf{P}$ are positive determined. The condition number $\mathrm{cond}(\mathbf{P}) = 1.03$ shows low sensitivity to inaccurate data. The SAFLC system is stable for all possible changes in references, disturbances and parameters of the plant and of the controllers in the ranges of adaptation. In no solution of (7) it is found the FLS is redesigned for greater plant changes.

6. **Conclusion and Future Research.** A novel systematic approach for a model-free design of a MIMO supervisor-based adaptive fuzzy logic controller is developed and illustrated for the coupled levels control in a two-tank system. An FLC system with empirically designed main MIMO Mamdani PI-FLC is investigated in real-time control. The data collected assist a MIMO TSK plant modeling using GAs error minimization. A MIMO FLS design is suggested on the basis of the FLC system sensitivity analysis. The real-time experimentation with the developed FLC-FLS system shows reduction of the settling time and the channels decoupling in comparison to the FLC system and also validates the TSK plant model. The Lyapunov system stability is studied using LMIs and the TSK-PDC system representation after a PDC GAs approximation of the FLC-FLS and a PDC validation from system real-time control data. The PDC of a smaller number of FUs and local PI controllers is simple and can be easily completed on PLCs thus facilitating its broad industrial application.

The future research will focus on the industrial application of the developed approach for levels control in carbonisation columns for the production of soda in order to increase the dynamic accuracy with smooth control and higher durability of the expensive actuators.

Acknowledgment. The investigation is supported by grant NIS-152pd000608/2015 of the Research Centre of the Technical University of Sofia.

REFERENCES

[1] T. Neshkov, S. Yordanova and I. Topalova, *Process Control and Production Automation*, TU, Sofia, 2007.
[2] D. Driankov, H. Hellendoorn and M. Reinfrank, *An Introduction to Fuzzy Control*, Springer-Verlag, NY, 1993.
[3] K. Passino and S. Yurkovich, *Fuzzy Control*, Addison-Wesley Longman, Inc., California, 1998.
[4] K. Astrom and B. Wittenmark, *Adaptive Control*, Addison-Wesley, 1989.
[5] O. Karasakal, E. Yesil, M. Guzelkaya and I. Eksin, Implementation of a new self-tuning fuzzy PID controller on PLC, *Turk. J. Elec. Eng.*, vol.13, no.2, pp.277-286, 2005.
[6] N. Kanagaraj, P. Sivashanmugam and S. Paramasivam, A fuzzy logic based supervisory hierarchical control scheme for real time pressure control, *Int. J. Autom. & Comp.*, vol.6, no.1, pp.88-96, 2009.
[7] K. D. Sharma, M. Ayyub, S. Saroha and A. Faras, Advanced controllers using fuzzy logic controller for performance improvement, *IEE Journal*, vol.5, no.6, pp.1452-1458, 2014.
[8] S. Soyguder and H. Alli, Fuzzy adaptive control for the actuators position control and modeling of an expert system, *Expert Syst. with Appl.*, vol.37, no.3, pp.2072-2080, 2010.
[9] S. Yordanova and V. Yankov, Fuzzy supervisor for nonlinear self-tuning of controllers in real time operation, *Proceedings of the Technical University of Sofia*, vol.64, no.1, pp.131-140, 2014.
[10] J. Jantzen, *Foundations of Fuzzy Control*, John Wiley & Sons, NY, 2007.
[11] Z. Li, Design of fuzzy neural network based control system for cement rotary kiln, *Informatics in Control, Automation & Robotics*, vol.2, pp.290-293, 2010.
[12] Q. Lu and M. Mahfouf, A model-free self-organizing fuzzy logic control system using a dynamic performance index table, *Transactions of the IMC*, vol.32, no.1, pp.51-72, 2010.
[13] O. Lutfy and E. Khduir, A PID-like ANFIS controller trained by PSO technique to control nonlinear MIMO systems, *Austr. J. of Basic and Appl. Sci.*, vol.7, no.4, pp.626-640, 2013.
[14] I. Rojas, H. Pomares, J. Gonzalez, L. J. Herrera, A. Guillen, F. Rojas and O. Valenzuela, Adaptive fuzzy controller: Application to the control of the temperature of a dynamic room in real time, *Fuzzy Sets & Syst.*, vol.157, no.16, pp.2241-2258, 2006.
[15] C. Treesatayapun, Balancing control energy and tracking error for fuzzy rule emulated adaptive controller, *Appl. Intell.*, vol.40, no.4, pp.639-648, 2014.
[16] O. Aydogdu and O. Alkan, Adaptive control of a time-varying rotary servo system using a fuzzy model reference learning controller with variable adaptation gain, *Turkish J. of Electr. Eng. & Comp. Sci.*, vol.21, no.2, pp.2168-2180, 2013.
[17] O. Cerman and P. Hussek, Fuzzy model reference learning control with modified adaptation mechanism, *Proc. of the 7th IEEE Int. Conf. on Natural Computation*, Shanghai, China, pp.123-128, 2011.
[18] Y.-W. Cho, K.-S. Seo and H.-J. Lee, A direct adaptive fuzzy control of nonlinear systems with application to robot manipulator tracking control, *Int. J. Control, Autom & Syst.*, vol.5, no.6, pp.630-642, 2007.
[19] A. G. Ram and S. A. Lincoln, A model reference-based fuzzy adaptive PI controller for non-linear level process system, *Int. J. Research and Reviews in Appl. Sci.*, vol.14, no.2, pp.477-486, 2013.
[20] H.-X. Li and S. K. Tso, A fuzzy PLC with gain-scheduling control resolution for a thermal process – A case study, *Control Eng. Practice*, vol.7, no.4, pp.523-529, 1999.
[21] Y. Pan and M. J. Er, Enhanced adaptive fuzzy control with optimal approximation error convergence, *IEEE TFS*, vol.21, no.6, pp.1123-1132, 2013.
[22] Y. Pan, H. Yu and T. Sun, Global asymptotic stabilization using adaptive fuzzy PD control, *IEEE Trans. Cybernetics*, vol.45, no.3, pp.588-596, 2015.
[23] A. Ghaffari, A. H. Shamekhi, A. Saki and E. Kamrani, Adaptive fuzzy control for air-fuel ratio of automobile spark ignition engine, *Proc. of World Academy of Sci., Eng. & Techn.*, vol.48, pp.284-292, 2008.
[24] R. K. Mudi and N. R. Pal, A self-tuning fuzzy PI controller, *Fuzzy Sets & Syst.*, vol.115, no.2, pp.327-338, 2000.
[25] C.-J. Wu, C.-N. Ko, Y.-Y. Fu and C.-H. Tseng, A genetic-based design of auto-tuning fuzzy PID controllers, *Int. J. Fuzzy Syst.*, vol.11, no.1, pp.49-58, 2009.

[26] J. Zheng, S. Zhao and S. Wei, Application of self-tuning fuzzy PID controller for a SRM direct drive volume control hydraulic press, *Contr. Eng. Practice*, vol.17, no.12, pp.1398-1404, 2009.
[27] S. Yordanova and V. Yankov, Design and stability analysis of supervisor-based adaptive fuzzy logic control system for temperature, *Int. J. of IT, Eng. & Appl. Sci. Research*, vol.4, no.4, pp.20-29, 2015.
[28] *Fuzzy Logic Toolbox: User's Guide for Use with MATLAB*, MathWorks, Inc., Natick, 1998.
[29] *MATLAB – Genetic Algorithm and Direct Search Toolbox*, User's Guide, MathWorks, Inc., Natick, 2004.
[30] *SIMATIC S7 Fuzzy Control*, User's Manual, Siemens AG, 2001.
[31] Dharamniwas, D. Ahmad, A. Ahmad, V. Redhu and U. Gupta, Liquid level control by using fuzzy logic controller, *Int. J. of Advances in Eng. & Techn.*, vol.4, no.1, pp.537-549, 2012.
[32] B. Kumar and R. Dhiman, Optimization of PID controller for liquid level tank system using intelligent techniques, *Canadian J. on Electrical and Electronics Eng.*, vol.2, no.11, pp.531-535, 2011.
[33] S. Yordanova, Intelligent approaches to real time level control, *Int. J. Intell. Sys. & Appl.*, vol.7, no.10, pp.19-27, 2015.
[34] S. Yordanova, Fuzzy logic approach to coupled level control, *Systems Sci. and Control Engin. – An Open Access Journal*, vol.4, no.1, pp.215-222, 2016.
[35] K. Tanaka and H. Wang, *Fuzzy Control Systems Design and Analysis: A Linear Matrix Inequality Approach*, John Wiley & Sons, NY, 2001.